ASSIMILATION OF M8-AMV DATA IN THE HIRLAM-NWP MODEL

C. Geijo Guerrero [a] and B. Amstrup [b]
[a] Spanish Meteorological National Institute (INM); cgeijo@inm.es
[b] Danish Meteorological Institute (DMI);bja@dmi.dk

ABSTRACT

Atmospheric Motion Vectors (AMV) generated from M8 geostationary satellite images have been used to carry out observation usage experiments with the HIRLAM assimilation and short-range limited-area NWP system. The experiments have been performed at two different operational NWP centres within the HIRLAM consortium, the Danish Meteorological Institute (DMI) and the Spanish National Meteorological Institute (INM). The main target of these experiments has been to test the impact of some new features and enhancements incorporated to AMV data over recent past (e.g., new imagery data) on the quality of weather predictions. The results obtained at DMI indicate that M8-AMV data has a slight positive impact on this quality as measured with surface and upper-air in-situ observations from the EWGLAM stations list. This implies that geostationary AMV wind data can be accommodated in the data assimilation schedule, without necessarily expecting a degradation of the forecast skill scores, together with other polar satellite data (scatterometer sea-surface winds and AMSU-A temperature soundings) currently used at DMI. The results obtained at INM indicate that AMV data has a significant impact on the way the model simulates the Atmospheric Dynamics at middle and low latitudes over the Northern Hemisphere Atlantic Ocean, that this impact is positive and sizeable (about 20% geopotential error reduction for the +24 h forecast) when measured by verification with analysed fields, and that it is particularly clear at low and middle levels in the Troposphere.

Introduction

AMV data have been around for some time already. In the context of European Meteorology from geostationary orbit, the generation of this kind of data started soon afterwards the launch of the first METEOSAT in November 1977. Today, all major operators of geostationary meteorological satellites include tracking vectors in their products catalogues, providing so with global coverage at low and middle latitudes, and these data are routinely monitored and assimilated by many NWP centres around the world. AMV constitute a reliable and well established source of wind data, and all indicates that it will also be so in the future. Since few years ago, a similar processing technique is used on data from imagers embarked on polar platforms (MODIS), extending the geographical coverage of these data to the whole globe. In the near future, hyperspectral data from geosynchronous satellites (e.g., GIFTS from USA) will very likely bring in qualitative changes. The opportunity of the experiments described in this communication arises from the consideration that the arrival of new radiometers (e.g., SEVIRI) is indeed a good occasion to revisit AMV data assimilation routines. This work does not deal with data from other systems able to measure wind from space, like scatterometer and new lidar (e.g., ADM-Aeolus, ESA) instruments.

The assimilation schemes used operationally in NWP have experienced significant changes and improvements over the last years. In the context of HIRLAM, this effort has led to the substitution of outdated Optimal Interpolation assimilation algorithms for global spectral statistical interpolation methods, usually known as 3D-Var (Parrish and Derber, 1992), and to the implementation of even more sophisticated algorithms based on "Control Theory" (Lions, 1971), usually known as 4D-Var. This terminology seems to indicate that between these two schemes there is an ordinal relationship, and in fact this impression is not totally wrong. The 3D-Var algorithm is a convenient previous step towards the implementation of the 4D-Var algorithm. Both pose the data assimilation problem as a variational problem, the former uses model fields as a weak constraint to solve this problem, while the latter uses a simplified version of the model dynamics as a strong constraint to find an analysis. With an eye put on one topic of great interest to HIRLAM, namely mesoscale NWP, these constraints have been recently re-formulated in order to make them flexible enough to account for model error structures that can arise in the mesoscale and that do not let themselves be easily expressed in an analytical form. This new formulation of these constraints is known as "statistical" (Berre, 2000). This communication intends to add some more elements for the assessment of the performance of these new developments.

The M8-AMV data

The AMV vectors used in these experiments were generated from sequences of M8-SEVIRI images in four different spectral bands: 0.8, 6.2, 7.3 and 10.8 microns at a nominal spatial resolution of 72 Km. These vectors were produced at a rate of 24 times a day with nominal observation times 00:30Z, 01:30Z, ...,23:30Z. The product generator (http://www.eumetsat.int) provides, together with the horizontal wind and wind height measurements, a certain amount of additional information including: vector type, height assignment method used, correlation method used, intermediate (15 minutes) relative displacement vectors, auxiliary information related to the height assignment process and quality confidence indexes. In these experiments most of this additional information was not considered, with the exception of the quality confidence indexes that were employed for the screening and thinning of the AMV data.

The HIRLAM NWP system

For the sake of brevity, I will present the NWP system used in these experiments in a very concise way. These experiments have been performed with the NWP system HIRLAM (High Resolution Limited Area Model; http://hirlam.knmi.nl) version 6.3.6. In its present status, the core of this system consists of an assimilation module which can be configured for different algorithms, and an atmosphere primitive equations hydrostatic model coupled to a land-surface scheme known as ISBA (Interaction-Soil-Biosphere-Atmosphere). The system can represent properly physical processes like transfer of radiation energy through the atmosphere, water cycle in the atmosphere (i.e., condensation and precipitation), convention and turbulence. The system offers as well different possibilities as far as adiabatic formulation of equations and the balancing of analysed fields is concerned. Geographical domain and space-time resolutions are equally configurable.

Tuning of HIRLAM 3D-Var for AMV assimilation

Previous to the assimilation experiments some work was done on M8-AMV data monitoring and on tuning of parameters that determine the screening of these data and their weights in the analysis.

By plotting monthly mean (Feb-March 2005) wind speed difference between AMV observations and short-range forecasts on a 2D graph with the x-axis for quality index (QI) and the y-axis for height (not shown), one can quickly get an idea about at which levels and for which QI thresholds the presence of systematic differences can reasonably be ruled out. The vectors from the 0.8 microns channel over sea surface and QI above 0.8 or 0.85 correspond well with the flow in the model at levels between 800 and 950 hPa. The same applies to vectors from the 10.8 microns channel. A significant portion of these 10.8 vectors are assigned height levels between 450 and 200 hPa, where they show a negative bias of a few m/s. The QI discriminates the worst cases, but only in part. The vertical distribution of the number of vectors from the 7.3 microns channel presents two local maxima at about 600 and 300 hPa. QC values above 0.85 or 0.9 correspond to bias-free vectors in the lower set but not in the upper set, where the bias is of the same order as for the 10.8 microns vectors. Vectors from the 6.2 microns concentrate at levels between 450 and 200 hPa. The statistics for this month show that there is a negative bias here as well, although those near the 400 hPa are almost bias-free. The QI discriminates the worst cases only in part. This characterisation is based on the QI that does not include a preliminary check with short-range forecasts and cloudy and clear-sky water vapour vectors were treated on the same footing.

The quality control or screening process of single-level wind data in the 3D-Var HIRLAM system (Gustafsson et al., 2001) consists basically of three steps: background check, thinning and variational quality control. The background check compares observed wind and guessed wind interpolated in space and time to the location and nominal time of the observation. If the difference falls outside the range where the distribution departs clearly from normality the observation is rejected. Figure 1 illustrates the procedure. The empirical distribution of innovations (i.e., differences between short-range forecast and observations) have been transformed and fitted to a gaussian model (slant strait lines). Some distance away from the origin (vertical red line) the deviation between data and model is judged significant. The plot on the left corresponds to low level vectors and that on the right to high level vectors. It is found that a mean wind component difference of about 5 m/s for low level winds and about 10 m/s for high level winds are adequate background check rejection thresholds. These values are somewhat bigger than those set up by default in the system. Another feature of this background check is the so-called “asymmetry

check", a scheme that makes more stringent this background check when the observation speed is below the guessed speed by more than 4 m/s. This asymmetry check aims at removing the structure of the systematic difference usually found in AMV data and confirmed for M8-AMV data as well. This asymmetry check was suppressed for vectors below 700 hPa because these vectors seem to be free of this bias.

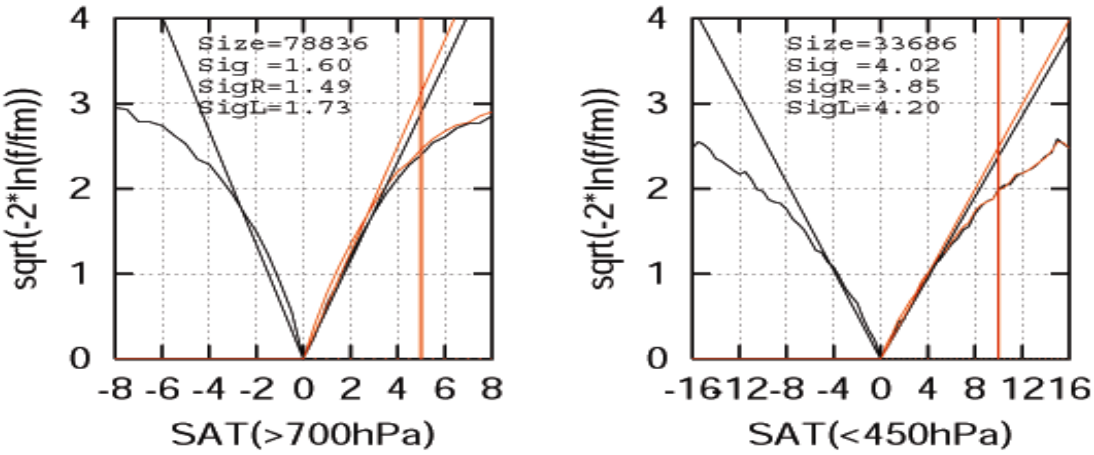

Figure 1. Determination of thresholds for the background check for AMV data (see text).

Dense wind fields are thinned up to minimise the effect of error correlation among nearby vectors (Bormann et al., 2002). In NWP data assimilation, errors of observations at different places are usually supposed uncorrelated. This simplification can be justified in practice because of the lack of information about how this correlation looks like and because it simplifies considerably the algebra. However, it is known that wrong specification of the error structure leads to "sub-optimal" analyses (Daley, 1991). One way to minimise this problem, and easy to implement, is by imposing a minimum separation between satellite observations. The obvious question is then how much thinning should be applied. The analysis error can be estimated by measuring the size of the "analysis residues", i.e., the distance between analysis and observations, therefore the question can be answered by studying the relationship between the degradation of the fit of the analysis to radio-sonde wind observations and the amount of thinning applied to the AMV vector fields.

Figure 2 summarises the results obtained from these tests. Five midday analysis were repeated five times each with decreasing intensity of thinning: maximum (i.e., no AMV data included), 1. degree minimum separation, 0.5 degrees, 0.3 degrees and 0.1 degrees. The minimum distance along the vertical was held fixed at 50 hPa. The radio-sonde wind data are from land-based stations south of 50 N. On the left, one can see the variation of the median of the distribution of the wind components normalised residues with the thinning intensity for the so-called "analytical formulation" of the background constraint, and on the right the corresponding results for the "statistical formulation" of this constraint. Each line corresponds to a different level in the atmosphere, as indicated by the legend included in the graphs. In the first case, the degradation in the quality of the analysis is apparent (particularly at high and medium levels) when the thinning is applied at or less than 0.5 degrees. In the second case, the curves show a different aspect, indicating much reduced sensitivity to the amount of thinning applied. Here, 0.5 seems one option quite conservative. We see as well that if AMV data is not assimilated, the characteristic size of the residues from both formulations are different: 0.41 (high level) and 0.26 (low and medium levels) for the analytical versus 0.34 and 0.21 for the statistical, this fact is a clear indication that the new formulation of the constraint works better than the older. This difference in the performance of both formulations is amplified when AMV data is introduced in the analysis. It is important to say that the differences seen in these graphs can not be attributed to problems with the converge of the minimisation algorithm. Converge is reached in all cases, although somewhat faster with the statistical formulation.

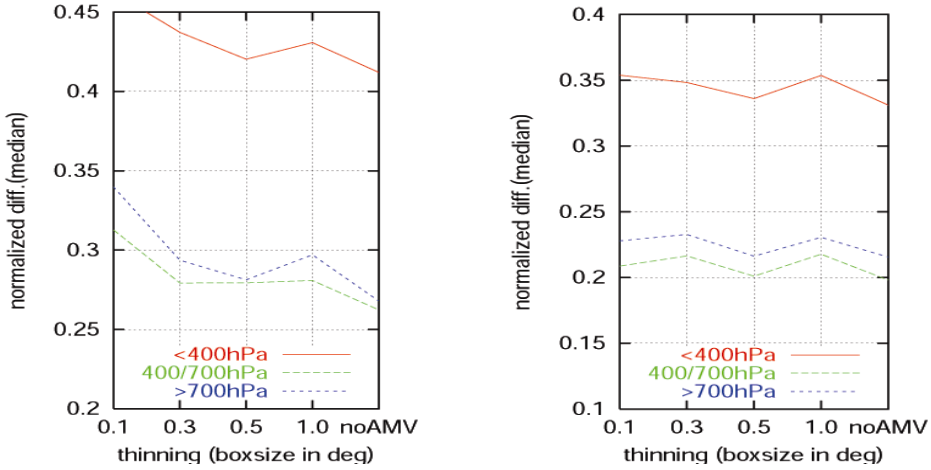

Figure 2. Determination of the amount of thinning for AMV data (see text)

The VarQC scheme (Anderson and Järvinen, 1999) solves the problem of quality control of observations from a bayesian approach. The scheme computes the "a posteriori" probability (P) of a given observation being affected by a "gross" or "non-normal" error, and this probability is then used to penalise the given observation if, as the iterative minimisation process progresses, the deviation between the observation and the updated background persists. The penalisation consists in decreasing the contribution of the given observation to the cost function gradient proportionally to (1-P).

The method assumes for the observational error the following error model: (1-A) $N(0,\sigma_o)$ + A $U(d,\sigma_o)$; where $N(0,\sigma_o)$ is the normal distribution, $U(d,\sigma_o)$ is the uniform distribution in the range $[-d\sigma_o , d\sigma_o]$, and A is the "a priori" probability of non-normal error in the observation. As shown in the reference, this "a priori" can be estimated by fitting the empirical distribution of normalised residues of the analysis to this error model. The Bayes theorem is then used to obtain the "a posteriori" probability from the "a priori" probability. It turns out that this fit is extremely sensitive to the standard observation error assigned to the observation type under consideration (in this case AMV data). The graph on the left of figure 3 illustrates this point. The red (low level vectors) and blue (high level vectors) lines are practically vertical, rendering the estimates of the "a priori"s very uncertain. It was found that fitting the error model to the tails of the distribution, rather than to the core of it as the first method does, gives more robust results. The lines drawn in the graph on the right of figure 3 show more elasticity and make it possible a more precise estimation of these probabilities.

From the x-axis of figure 3 one can quickly read out the maximum value of σ_o for which we obtain meaningful values of these "a priori"s (i.e., positive values). It is found that, for the current settings (σ_o=2 m/s at low levels, σ_o =5 m/s at high levels), the VarQC scheme has only a marginal impact on the assimilation of AMV data.

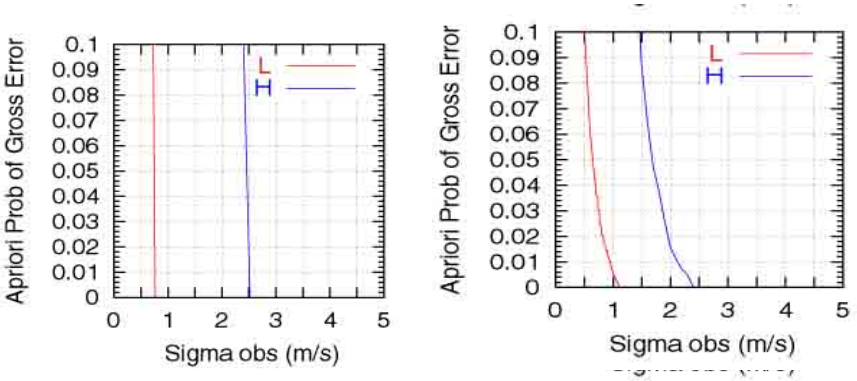

Figure 3. Determination of "A priori probabilities of gross error" for AMV data (see text)

Observation Usage Experiments at DMI

Several impact studies (unpublished results) with the DMI-HIRLAM analysis and forecasting system have in the past shown a very clear negative impact of using SATOB data. However, the last impact study with this kind of data was made around 2000 and since then a lot of progress in the production of these data has been made by satellite data providers. In addition, the new instrument SEVIRI on M8 has also made it possible to further improve the height assignment of these vectors in comparison with older METEOSAT satellites. In connection to the launch of M8, the necessary changes to use M8-AMV data were implemented in the HIRLAM 3D-Var/4D-Var analysis. This implementation makes it possible to use the quality indicators provided with the data.

The analysis algorithm used here is the HIRLAM 3D-Var 6.3.6 OpenMP version for NEC computers, modified to use RTTOV8 developed in the NWP-SAF. The observation time window covers a 3 hours span around the analysis times (00,03,...,21UTC) except for a 6 hours span around the analyses at times 06 and 18 UTC from which a long integration is launched. The standard observation set used includes: synoptic observations, ship observations, buoys (drifting and moored), pilot balloons, radio-sonde data, aircraft data, QuickScat and NOAA15/NOAA16 AMSU-A data. The experiments have been carried out over two operational DMI-HIRLAM areas. The "Global" area (DMI-HIRLAM-G) and the "European" area (DMI-HIRLAM-E). Both domains have a vertical resolution of 40 levels while the horizontal resolution is 0.45 degrees for the "G" model and 0.15 degrees for the "E" model.

The results obtained from an experiment run during January 2005 are shown in figure 4. The forecast skill scores are computed from co-locations with surface and upper-air measurements of pressure, wind, temperature, humidity and geopotential gathered from the EWGLAM stations list. The red (G4F) and green (D1F) lines correspond to the control integration (excluding M8-AMV data) for the global and European areas respectively. The blue (G4C) and black (D1C) lines correspond to the experiment integration (with M8-AMV data). Bias and r.m.s are plotted together on the same graphs .vs. forecast range. We can see that the impact has the same sign on both areas and that this impact is visible and positive for most of the parameters.

Based on the results from last year and the present results, M8-AMV data became part of the DMI operational suite on May 31, 2005.

Observation Usage Experiments at INM

The experiment described in this section was designed to evaluate the impact of M8-AMV data in a context of short-range forecasts (up to 24 hours) and short 3D-Var assimilation cycles (3 hours). This short assimilation cycle could reveal some of the potential of the high temporal resolution offered by these AMV data.

The period of time selected was 15/02/2005-15/03/2005. This choice arises from the interest in testing the impact under weather synoptic situations characterised by frequent transits of baroclinic disturbances. During that time a few of these events actually took place. Previous experiments carried out for Boreal Summer typical weather conditions (July 2003) over the same geographical area, indicated that assimilation of AMV data has a clear impact on the way the model reproduces atmospheric circulation regimes characterised by its persistence, e.g. trade winds (see figure 5).

The integrations were done at 0.2 degrees horizontal resolution and 40 vertical levels (hybrid vertical coordinates). The upper-air data assimilation time window spanned three hours, from two hours before nominal analysis time (0, 3,...21 UTC) until one hour after this time. For each assimilation cycle three AMV slots were used at -1h30m –30m and +30m from the nominal analysis time. For the calculation of innovations, the background was linearly interpolated to these times. The iterative minimisation process run smoothly, convergence was found in all cases before the maximum number of iterations allowed (100) could be reached. The variational quality control filter was activated at iteration number 20. The analysis of surface variables was done every six hours (0,6,12,18 UTC) using an OI algorithm. Residual imbalances in the analyses are suppressed by using DFI methods. ECMWF operational analyses were used as boundary conditions with a refreshing cycle of six hours.

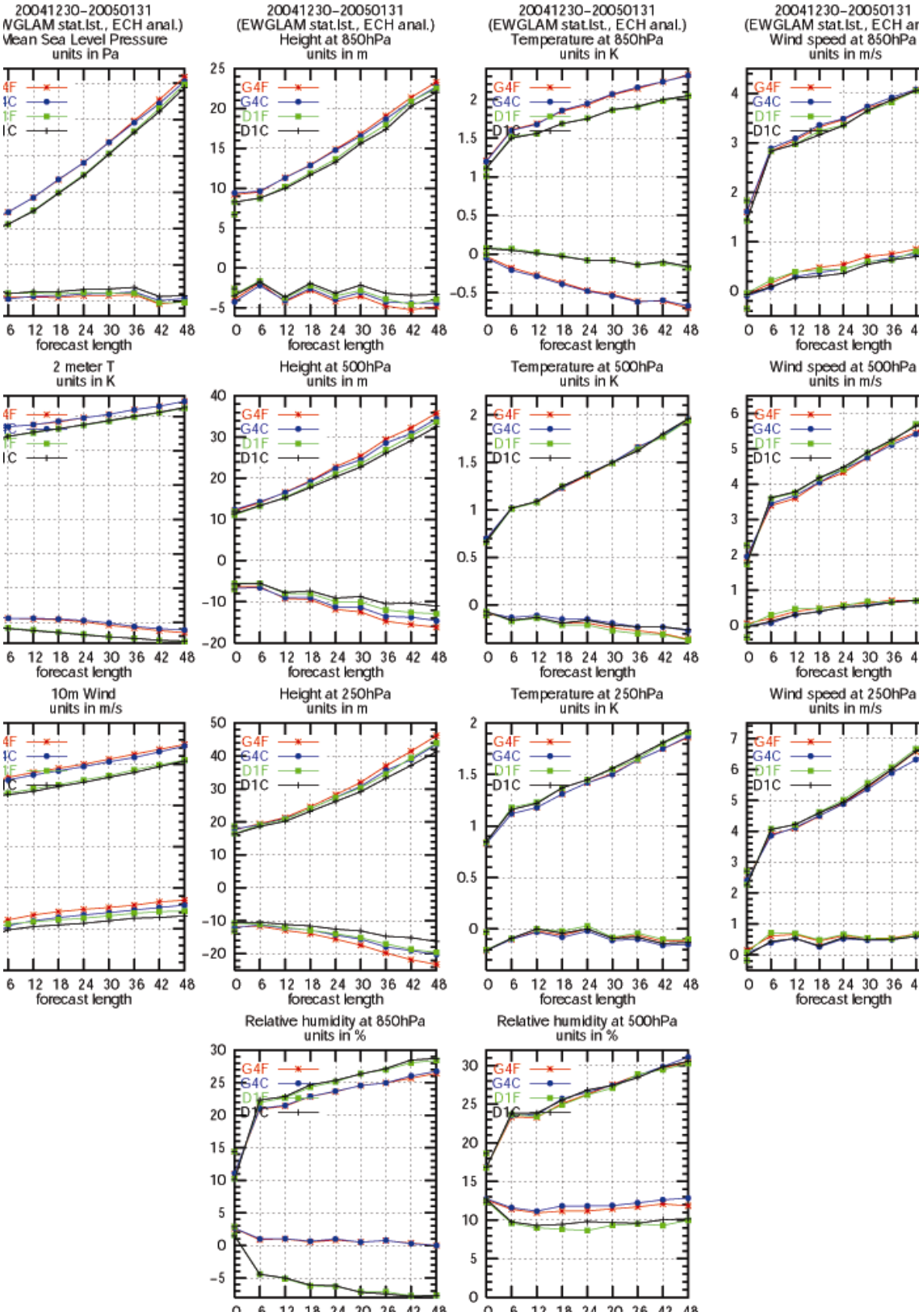

Figure 4. Impact on the forecast skill scores for the experiments carried out with DMI-HIRLAM-G (red for CNTL and blue for +AMV) and DMI-HIRLAM-E (green for CNTL and black for +AMV). (see text).

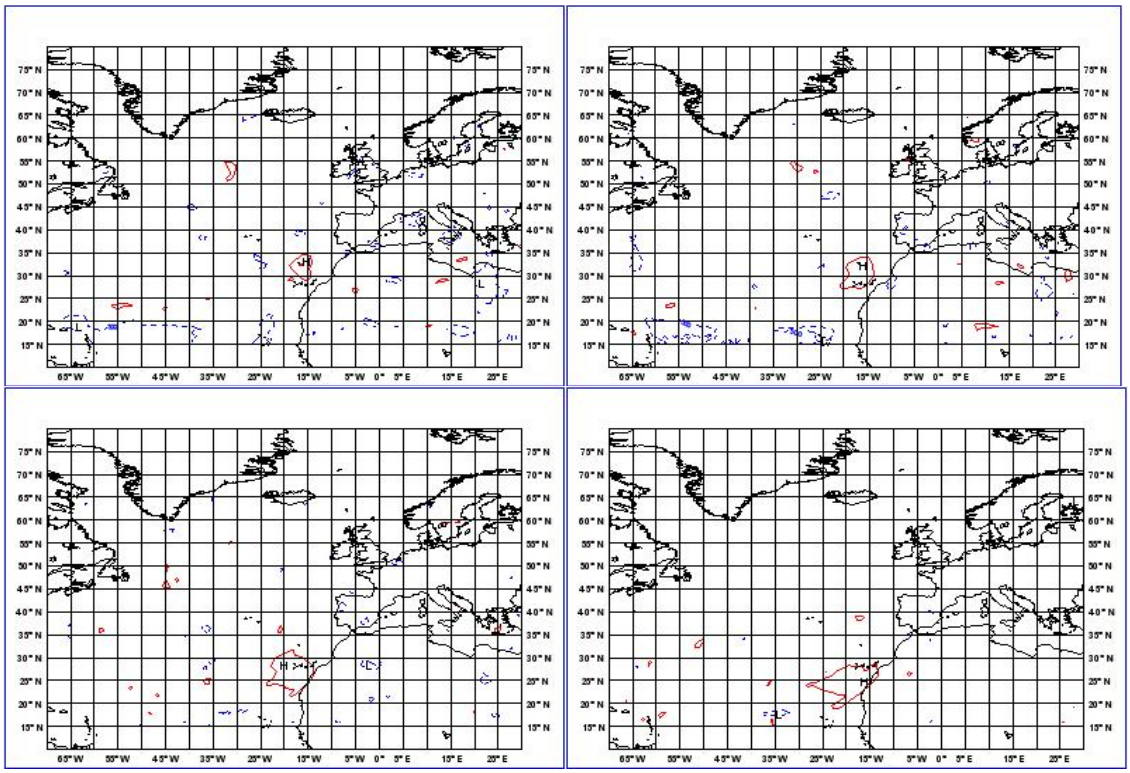

Figure 5. Impact of M7-AMV data over the Northern Subtropical Atlantic (July 2003). The maps correspond to wind speed at model level 28 (about 850 hPa). The red areas indicate the zones where the impact on the monthly mean wind speed is significant at 0. 5% level. Upper left panel is for analysis, upper right +6 hours forecast, +24 is down on the left and +48 hours down on the right. The monthly mean difference is about +1 m/s enhanced in the experiment.

Control and experiment configurations shared the same settings with the exception of two aspects: AMV data observation usage (absent in the control run) and the background constraint used. The control analyses were obtained with the old analytical formulation while the statistical formulation was employed for the experiment analyses. The observations common to both integrations are those that may be referred to as "terrestrial observations", i.e.: wind, temperature, pressure and humidity measurements taken from land and sea-surface based equipment, radio-sondes, balloons and aircrafts. In the experiment run, AMV data were not assimilated over land for latitudes above 35 degrees North. AMV data with quality index (without FG check) below 80 were equally discarded, independently of vector type or level. Rejection thresholds were given in agreement with the settings shown above (see "calibration of the assimilation algorithm"). The AMV data fields were thinned up down to 0.5 degrees and 50 hPa by picking up those vectors closest in time to the nominal analysis time or, if simultaneous, those with higher quality index.

The verification of the impact with "in-situ" observations (i.e., land-based stations and radio-sondes) was performed in a way that could enhance the visibility of its geographical distribution. Statistics of the comparisons between model and observations were produced and the sign and statistical significance of this impact were determined for each station. The three basic statistics worked out were: bias, r.m.s, and Spearman rank correlation (S, σ, Rs). For a given station, positive significant impact on the mean error or on the r.m.s is found when $S(exp) < S(cntl)$ or $\sigma(exp) < \sigma(cntl)$ at the 5% confidence level respectively. Positive impact is found for the Rs statistic when Rs(exp) is significant at 5% c.l. but not Rs(cntl). Negative impacts are found in opposite situations. Otherwise the impact is labelled as neutral.

Table 1 summarises the +24 hours forecast verification results for some surface variables: m.s.l pressure, wind speed and wind direction at 10 meters. Each row corresponds to a different spatial aggregate of stations: 1) the whole Iberian Peninsula and South of France, 2) the Gibraltar Strait area, 3) the Iberian Mediterranean Coast, 4) the Iberian North Coast, 5) the Iberian West Coast, 6) the Iberian South-western Coast and 7) the South of France. In each cell of the table two numbers appear side by side. The one on the left is the number of cases where positive impact was detected, the one on the right is the number of cases with negative impact. The reader can quickly grasp the sign and statistical significance of the

impact by comparing both numbers. We can notice an overall (i.e., whole Iberian Peninsula) positive impact on the bias for m.s.l pressure parameter, particularly over Gibraltar, Western and South-Western coasts. We can notice as well, on the other hand, a somewhat smaller negative impact on the r.m.s for wind direction at 10 m, distributed quite uniformly over the whole verification area of interest. It may be opportune to mention at this point that the FG check on wind direction was not activated for AMV data. The impact on wind speed is clearly neutral. The results for the upper-air variables (not shown) can be processed and presented in a similar way. It turns out that the impact is neutral.

Parameter	***Pmsl***			***Wind Speed 10m***			***Wind Direction 10m***		
	B	σ.	Rs	B	σ.	Rs	B	σ.	Rs
Iberian Peninsula	115;10	16 ; 19	0 ; 0	0 ; 0	1 ; 2	53 ; 46	0 ; 0	4 ; 50	49 ; 60
Gibraltar Strait Area	13 ; 0	1 ; 0	0 ; 0	0 ; 0	0 ; 0	5 ; 4	0 ; 0	0 ; 9	3 ; 5
Mediterranean Coast	0 ; 0	0 ; 0	0 ; 0	0 ; 0	0 ; 0	13 ; 10	0 ; 0	0 ; 7	20 ; 6
North Coast	6 ; 1	1 ; 10	0 ; 0	0 ; 0	0 ; 0	1 ; 2	0 ; 0	0 ; 0	1 ; 0
West Coast	41 ; 4	1 ; 0	0 ; 0	0 ; 0	0 ; 0	3 ; 4	0 ; 0	0 ; 4	4 ; 6
South-West Coast	15 ; 0	1 ; 0	0 ; 0	0 ; 0	0 ; 0	1 ; 1	0 ; 0	0 ; 8	2 ; 4
South of France	0 ; 0	0 ; 7	0 ; 0	0 ; 0	0 ; 0	2 ; 5	0 ; 0	1 ; 11	2; 4

Table 1 Summary of the impact verification results with in-situ surface observations over the Iberian Peninsula and nearby areas (see text).

An alternative way of evaluating the impact is by comparing forecasted fields and analysed fields at the corresponding verification times. One obvious drawback of this method is that it does not provide with a unambiguous reference for verification because two sets of analyses are available, those produced by the control and those originated from the experiment. These analysis may differ because they originate from different observations and, as is the case here, from different methods as well. One simple way around this difficulty is to verify each integration with its own analyses. It is then possible to see if the model propagates the information introduced in the system by the new data consistently. When this is actually what happens, our confidence in the positive impact of the data being tested rises. If this consistency is not found, the analysis of the results should give hints about possible problems with the data under consideration. This information is certainly very useful at the time of establishing an assimilation strategy for these data.

Figure 6. (top) shows the spatial distribution of the difference between control and experiment r.m.s error for the +24 hours forecast 500 hPa geopotential height parameter, i.e, the spatial distribution of:

$$VP = \sigma\,(fc(+24)\text{-}an)_{cntl} - \sigma\,(fc(+24)\text{-}an)_{exp}$$

Solid lines, where the difference is positive, indicate a positive impact, i.e., the error in the control integration is bigger than in the experiment integration. Dashed lines contour areas where the opposite situation occurs. The map corresponds to midday runs and is quite similar to those for other runs of the day (not shown). The shaded areas indicate monthly mean values of the baroclinic instability as measured by the Eady maximum growth rate index averaged over a layer bounded by surface and 300 hPa, i.e. these shaded areas indicate areas of maximum baroclinic activity during the period of the experiment. We can see that the positive impact is dominant at latitudes south of about 45 N and that these positive impact areas are located mainly downstream of high instability zones. This result suggests that these data can improve the simulation of the evolution of baroclinic structures, which is remarkable in the sense that assimilation algorithms tend to extrapolate single level data barotropically. The time series at the foot of the map corresponds to the spatial average of VP over an area west of 10W and south of 45N, i.e. over the area where the positive impact is more significant. The error reduction amounts to about 22%. These values are in line with results obtained by Gelaro et al. (2000) with the NOGAPS NWP system and data from the NORPEX (North Hemisphere Pacific Ocean) observation campaign. At the 850 hPa level, the results are similar with an error reduction of about 12% (not shown).

Figure 7 shows the spatial distribution of VP for geopotential height at 200 hPa. Around 0 degrees longitude and for latitudes between 45N and 25N, the introduction of AMV data degrades the agreement between the 24 hours forecasts and the analyses. This pattern can be seen as well in the spatial

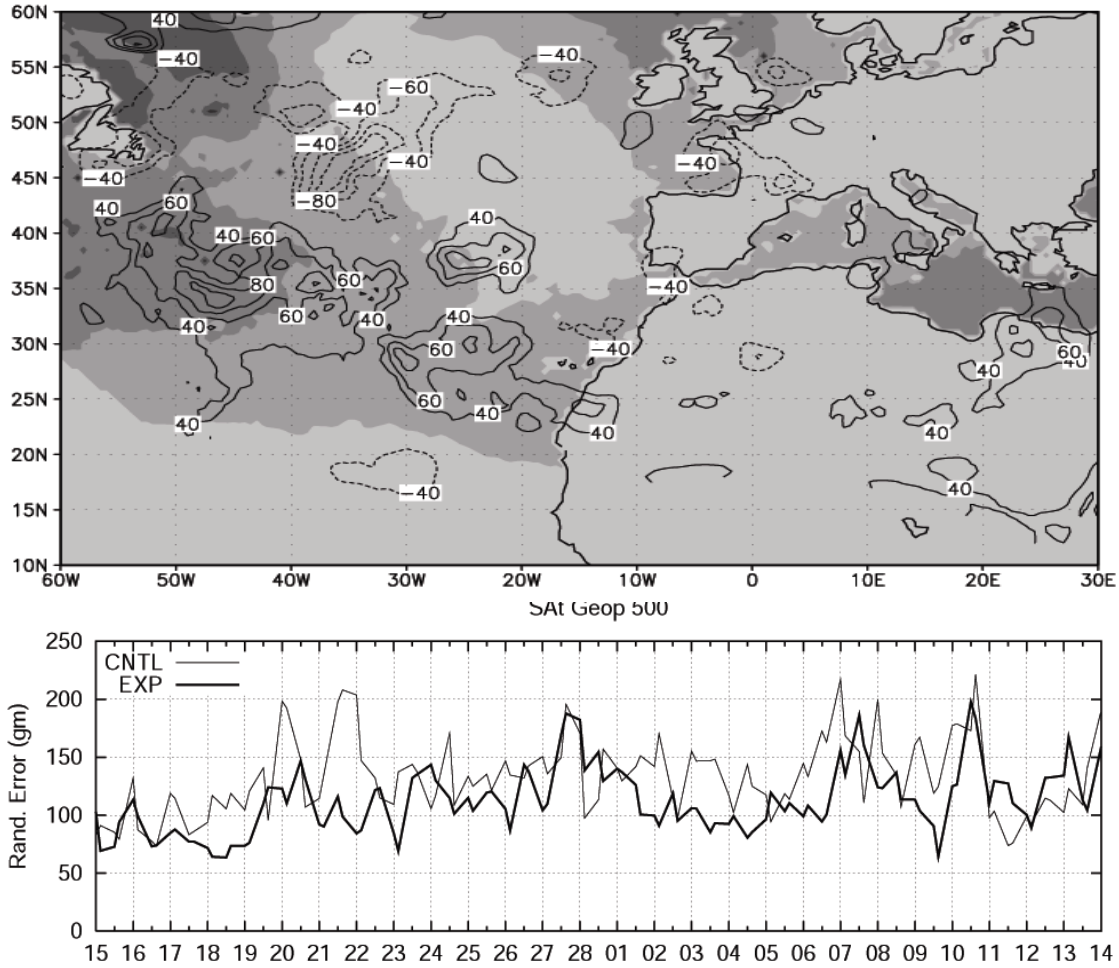

Figure 6. ***Top*****.- Spatial distribution of the impact on 500 hPa geopotential height verified using analyses.** ***Bottom*** **.- Time series for this impact averaged over the Atlantic South of 45 N (see text).**

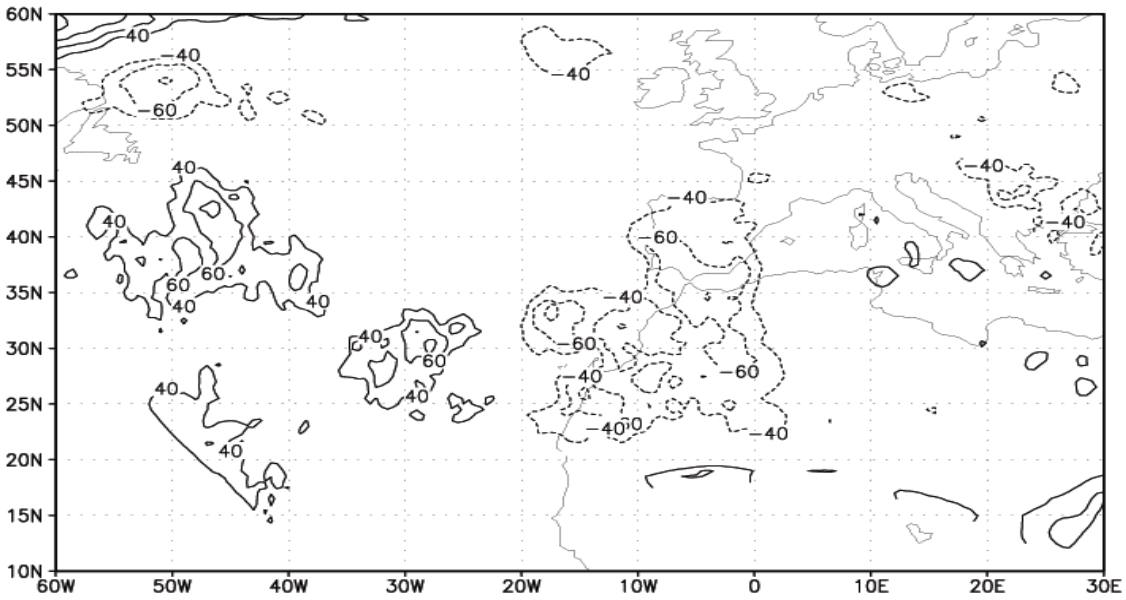

Figure 7.- Spatial distribution of the impact on 200 hPa geopotential height verified using analyses. (see text).

distribution of VP for other parameters like wind speed (not shown). This degradation may be caused by variability over a period of 24 hours in the height assigned to vectors that actually should correspond to the same level, in other words, it is possible to understand this effect as caused by uncertainty in the AMV reported level. The fact that the sign of the impact changes over the western part of the domain, where cloudy conditions predominated during the experiment, as opposed to clear sky conditions dominating the area where negative impact has been detected, suggests that this effect could be attributed to clear sky AMV data. However, this possibility has not been checked out in this study.

Conclusions

We have measured the impact of 3D-Var assimilation of M8-AMV data on the skill of short-range forecasts generated by the HIRLAM hydrostatic model (version 6.3.6). Verification with conventional "in-situ" surface and upper-air observations at a European Continental scale (EWGLAM stations list) over one month period (January 2005) show a small positive impact, and this advocates in favour of the assimilation in the DMI operational suite of M8-AMV data together with other data from polar meteorological satellites (ocean-surface wind data from QuickScat and temperature sounding data from NOAA15-NOAA16 AMSU-A). Verification with conventional "in-situ" surface and upper-air observations over the Iberian Peninsula for one month period (February-March 2005) gives an overall neutral impact with small improvement on the P_{msl} parameter and marginal negative impact on the 10 meters wind direction parameter. This marginal negative impact might have been caused by a relaxation in the data screening process. At any rate, these verifications based on "in-situ" data suffer from very low S/N ratios and can only be conclusive in the sense that the assimilation of M8-AMV does not perturb significantly the agreement between model and "in-situ" observations.

The impact has been measured as well in terms of consistency between forecasts and analyses generated by the own integration (control or experiment). Over the Northern Hemisphere Atlantic Ocean and south of about 45-50 degrees North, the use of AMV data produces a sizeable positive impact at low and medium levels in the Troposphere. In terms of geopotential height, this impact amounts to error reductions of 10%, 20% at 850 hPa, 500 hPa respectively for the 24 hours forecast range. The spatial structure of this impact indicates that this result is connected with a more precise description by the model of the transit of baroclinic instabilities across the Atlantic during the time period considered (February-March 2005). This result is in qualitative and quantitative agreement with other investigations carried out with NORPEX data over the Northern Hemisphere Pacific Ocean. This result complements as well other studies where the AMV data showed a clear impact on the way the model simulates the trade winds circulation , making it more intense by about 1 m/s in monthly mean. Therefore it seems fair to conclude that assimilation of AMV data has clear potential to impact and improve the simulation of Atmospheric Dynamics over the North Atlantic. It has been found as well problems with the assimilation of these AMV data at higher levels. The uncertainty in the height assigned to these vectors negatively impacts on the dispersion between forecasted and analysed model fields.

References

Andersson E. And Järvinen H., 1999; "Variational Quality Control". Q.J.R.Meteorol.Soc, **125**, 697-722.

Berre.L, 2000; "Estimation of Synoptic and Mesoscale Forecast Error Covariances in a Limited-Area Model",Mon.Wea.Rev, **128**, 664-667

Bormann N. et al. , 2002 ;"The Spatial Structure of Observation Errors in Atmospheric Motion Vectors". Proc Sixth. International Winds Workshop, Wisconsin, Madison, USA.EUMETSAT,EUM P 35, 113-120.

Daley R., 1991, "Atmospheric Data Analysis", Cambridge University Press.

Gelaro R. et al, 2000, "A Predictability Study Using Geostationary satellite Wind Observations during NORPEX", Mon. Wea. Rev., **128**, 3789-3807.

Gustafsson N. et al., 2001 "Three-dimensional Variational Data Assimilation for a Limited Area Model", Tellus, **53**, 425-446.

Lions,J.L,1971; Optimal Control of Systems Governed by Partial Differential Equations, Springer-Verlag, Berlin

Parrish D.F and Derber J.C, 1992, "The National Meteorological Center's Spectral Statistical Interpolation Analysis System", Mon.Wea.Rev.,**120**,1747-1763.